Correlating lepton flavor universality violation in B decays with $\mu \to e$ using leptoquarks

Crivellin, Andreas ; Müller, Dario ; Signer, Adrian ; Ulrich, Yannick

Abstract: Motivated by the measurements of b→s + − transitions, including R(K) and R(K∗), we examine lepton flavor (universality) violation in B decays and its connections to →e in generic leptoquark models. Considering all 10 representations of scalar and vector leptoquarks under the Standard Model gauge group we compute the tree-level matching for semileptonic b-quark operators as well as their loop effects in → . In our phenomenological analysis, we correlate R(K), R(K∗) and the other b→s + − data to →e and b→s e transitions for the three leptoquark representations that generate left-handed currents in b→s + − transitions and, therefore, provide a good fit to data. We find that while new physics contributions to muons are required by the global fit, couplings to electrons can be sizeable without violating the stringent bounds from →e . In fact, if the effect in electrons in b→s + − has the opposite sign from the effect in muons, the bound from →e can always be avoided. However, unavoidable effects in b→s e transitions (i.e. Bs→ e, B→K e, etc.) appear that are within the reach of LHCb and BELLE II.

DOI: https://doi.org/10.1103/physrevd.97.015019

Originally published at:
Crivellin, Andreas; Müller, Dario; Signer, Adrian; Ulrich, Yannick (2018). Correlating lepton flavor universality violation in B decays with $\mu \to e$ using leptoquarks. Physical review D, 97:015019.
DOI: https://doi.org/10.1103/physrevd.97.015019

Correlating lepton flavor universality violation in B decays with $\mu \to e\gamma$ using leptoquarks

Andreas Crivellin*
Paul Scherrer Institut, CH–5232 Villigen PSI, Switzerland

Dario Müller,† Adrian Signer,‡ and Yannick Ulrich§
Paul Scherrer Institut, CH–5232 Villigen PSI, Switzerland and Physik-Institut, Universität Zürich, Winterthurerstrasse 190, CH-8057 Zürich, Switzerland

(Received 4 July 2017; published 29 January 2018)

Motivated by the measurements of $b \to s\ell^+\ell^-$ transitions, including $R(K)$ and $R(K^*)$, we examine lepton flavor (universality) violation in B decays and its connections to $\mu \to e\gamma$ in generic leptoquark models. Considering all 10 representations of scalar and vector leptoquarks under the Standard Model gauge group we compute the tree-level matching for semileptonic b-quark operators as well as their loop effects in $\ell \to \ell'\gamma$. In our phenomenological analysis, we correlate $R(K)$, $R(K^*)$ and the other $b \to s\mu^+\mu^-$ data to $\mu \to e\gamma$ and $b \to s\mu e$ transitions for the three leptoquark representations that generate left-handed currents in $b \to s\ell^+\ell^-$ transitions and, therefore, provide a good fit to data. We find that while new physics contributions to muons are required by the global fit, couplings to electrons can be sizeable without violating the stringent bounds from $\mu \to e\gamma$. In fact, if the effect in electrons in $b \to s\ell^+\ell^-$ has the opposite sign from the effect in muons, the bound from $\mu \to e\gamma$ can always be avoided. However, unavoidable effects in $b \to s\mu e$ transitions (i.e. $B_s \to \mu e$, $B \to K\mu e$, etc.) appear that are within the reach of LHCb and BELLE II.

DOI: 10.1103/PhysRevD.97.015019

I. INTRODUCTION

The LHC completed the Standard Model (SM) of particle physics by discovering the Higgs boson, but it did not yet directly observe any particles beyond the ones already present in the SM. However, several measurements of $b \to s\mu^+\mu^-$ transitions in recent years have lead to a tension with SM predictions. Due to an intriguing pattern in these anomalies, it is tempting to interpret them as an indirect hint for new physics (NP) [1–3]. Taking this approach and including the new LHCb result [4] for $R(K^*) = (B \to K^*\mu^+\mu^-)/(B \to K^* e^+e^-)$, measuring lepton flavor universality (LFU) violation, the global significance for NP increased above the 5σ level [5]. In addition, the combination of the ratios $R(D^{(*)}) = (B \to D^{(*)}\tau\nu)/(B \to D^{(*)}\ell\nu)$ also differs by 3.9σ from its SM prediction [6]. All together, this strongly motivates us to examine LFU violation in semileptonic B decays in the context of NP.

Since $b \to s\ell^+\ell^-$ processes are semileptonic, leptoquarks (LQ) provide a natural explanation for these anomalies (see, for example, [7–17]): They give tree-level contributions to these processes but contribute, for example, to $\Delta F = 2$ processes only at the loop level, therefore respecting the bounds from other flavor observables. Furthermore, since in $R(D^{(*)})$ an $\mathcal{O}(10\%)$ effect compared to the tree-level SM is needed, a NP tree-level effect is also required. Here, LQ are probably the most promising solution (see for example [8,17–26]). In fact, in Ref. [15], a model for a simultaneous explanation of $b \to s\mu^+\mu^-$ data together with $R(D^{(*)})$ has been proposed which is compatible with the bounds from $B \to K^{(*)}\bar{\nu}\nu$, electroweak precision data [27] and direct LHC searches [28]. Interestingly, LQ also provide a natural solution to the anomaly in the magnetic moment of the muon due to the possible enhancement by m_t/m_μ through an internal chirality flipping [19,29–32].

The model independent fit to $R(K)$ and $R(K^*)$ allows for NP contributions to electrons or muons separately, but also to both simultaneously [33–37]. Once the other data on $b \to s\mu^+\mu^-$ is included, NP in muons is required but is only optional for electrons. However, the best-fit value suggests a simultaneous NP contribution to electrons as well [5,33,38]. It is well known that once LQ couple to muons

*andreas.crivellin@cern.ch
†dario.mueller@psi.ch
‡adrian.signer@psi.ch
§yannick.ulrich@psi.ch

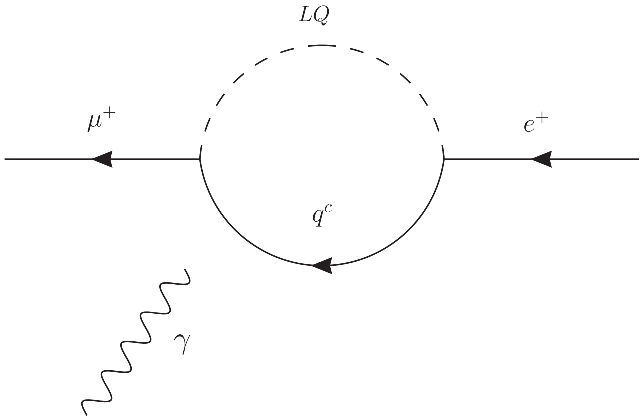

FIG. 1. Feynman diagram generating $\mu \to e\gamma$ in models with leptoquarks.

and electrons simultaneously, they give rise to lepton flavor violating B decays and to $\mu \to e\gamma$ [10] (see Fig. 1).

Both $\mu \to e\gamma$ and lepton flavor violating B decays with μe final states are experimentally very interesting, and precise upper limits for these processes already exist. For $\mu \to e\gamma$, the current experimental bound, obtained by the MEG Collaboration [39], is

$$\mathrm{Br}[\mu \to e\gamma] \leq 4.2 \times 10^{-13}, \tag{1}$$

and MEG II [40] at the Paul Scherrer Institute (PSI) will significantly improve on this bound in the future. Concerning lepton flavor violating B decays with μe final states, the current limits are [41]

$$\begin{aligned} \mathrm{Br}[B^+ \to K^+\mu^\pm e^\mp]_{\mathrm{exp}} &\leq 9.1 \times 10^{-8}, \\ \mathrm{Br}[B \to K^*\mu^\pm e^\mp]_{\mathrm{exp}} &\leq 1.4 \times 10^{-6}, \\ \mathrm{Br}[B_s \to \mu^\pm e^\mp]_{\mathrm{exp}} &\leq 1.2 \times 10^{-8}. \end{aligned} \tag{2}$$

Also here, LHCb and BELLE II will improve on these bounds in the near future.

In this article, we examine the interplay between $b \to s\mu^+\mu^-$ processes, $R(K^{(*)})$, $\mu \to e\gamma$ and $b \to s\mu e$ processes in detail considering LQ. For this purpose, we will take into account all 10 representations for scalar and vector LQ under the SM gauge group.

The article is structured as follows: In the next section, we will fix our conventions for the LQ interactions and calculate the contributions to $b \to s\ell^+\ell^-$ transitions and $\mu \to e\gamma$. We use these results in Sec. II to perform a phenomenological analysis for the three LQ representations that give a good fit to $b \to s\mu^+\mu^-$, considering the most constraining processes with electrons and muons in the final state. In Sec. IV, we briefly comment on τ-e and τ-μ transitions before we conclude. The Appendix presents the complete tree-level matching of the 10 LQ representations for semileptonic B decays (see also Ref. [11,42]) and their contributions to all $\ell \to \ell'\gamma$ processes.

II. MODEL AND OBSERVABLES

The possible representations of LQ under the SM gauge group were first categorized in Ref. [43]. There are five scalar LQ with the following quantum numbers:

$$\begin{aligned} Q(\Phi_1)&\colon \left(3, 1, -\frac{2}{3}\right), \\ Q(\tilde{\Phi}_1)&\colon \left(3, 1, -\frac{8}{3}\right), \\ Q(\Phi_2)&\colon \left(\bar{3}, 2, -\frac{7}{3}\right), \\ Q(\tilde{\Phi}_2)&\colon \left(\bar{3}, 2, -\frac{1}{3}\right), \\ Q(\Phi_3)&\colon \left(3, 3, -\frac{2}{3}\right) \end{aligned} \tag{3}$$

under the SM gauge group $SU(3)_C \times SU(2)_L \times U(1)_Y$, respectively. These new scalars couple to SM fermions in the following way:

$$\begin{aligned} \mathcal{L}_{\mathrm{scalar}}^{\mathrm{LQ}} = {} & (\lambda_{fi}^{1R}\overline{u_f^c}\ell_i + \lambda_{fi}^{1L}\overline{Q_f^c}\mathrm{i}\tau_2 L_i)\Phi_1^\dagger \\ & + \tilde{\lambda}_{fi}^{1}\overline{d_f^c}\ell_i\tilde{\Phi}_1^\dagger + \tilde{\lambda}_{fi}^{2}\overline{d_f}\tilde{\Phi}_2^\dagger L_i \\ & + (\lambda_{fi}^{2RL}\overline{u_f}L_i + \lambda_{fi}^{2LR}\overline{Q_f}\mathrm{i}\tau_2\ell_i)\Phi_2^\dagger \\ & + \lambda_{fi}^{3}\overline{Q_f^c}\mathrm{i}\tau_2(\tau\cdot\Phi_3)^\dagger L_i + \mathrm{H.c.} \end{aligned} \tag{4}$$

Here we assumed that lepton number and/or baryon number is conserved. This forbids couplings of LQ to two quarks (which are in principle allowed by gauge invariance) and ensures the stability of the proton.

Concerning vector LQ there are also five representations under the SM gauge group with charges

$$\begin{aligned} Q(V_1^\mu)&\colon \left(\bar{3}, 1, -\frac{4}{3}\right), \\ Q(\tilde{V}_1^\mu)&\colon \left(\bar{3}, 1, -\frac{10}{3}\right), \\ Q(V_2^\mu)&\colon \left(3, 2, -\frac{5}{3}\right), \\ Q(\tilde{V}_2^\mu)&\colon \left(3, 2, \frac{1}{3}\right), \\ Q(V_3^\mu)&\colon \left(3, 3, \frac{4}{3}\right). \end{aligned} \tag{5}$$

These new massive vectors couple to fermions via

$$\begin{aligned}\mathcal{L}^{\rm LQ}_{\rm vector} = &(\kappa^{1L}_{fi}\bar{Q}_f\gamma_\mu L_i + \kappa^{1R}_{fi}\bar{d}_f\gamma_\mu \ell_i)V_1^{\mu\dagger}\\ &+\tilde{\kappa}^{1}_{fi}\bar{u}_f\gamma_\mu\ell_i\tilde{V}_1^{\mu\dagger} + \tilde{\kappa}^{2}_{fi}\bar{u}^c_f\gamma_\mu\tilde{V}_2^{\mu\dagger}L_i\\ &+(\kappa^{2RL}_{fi}\bar{d}^c_f\gamma_\mu L_i + \kappa^{2LR}_{fi}\bar{Q}^c_f\gamma_\mu\ell_i)V_2^{\mu\dagger}\\ &+\kappa^3_{fi}\bar{Q}_f\gamma_\mu(\tau\cdot V_3^\mu)L_i + \text{H.c.}\end{aligned} \tag{6}$$

Again, we assume the conservation of lepton and baryon number. Even though massive vector bosons are not renormalizable without a Higgs mechanism, we will not specify the scalar sector. As we will see later, this is not necessary for our purpose because the new Higgs sector can be decoupled. We point out that this only works because $\ell \to \ell'\gamma$ is finite in unitary gauge.

Let us now turn to the calculation of the most relevant observables, $b\to s\mu^+\mu^-$, $b\to se^+e^-$, $b\to s\mu e$, and $\mu\to e\gamma$. For reasons explained at the end of this section we set the right-handed couplings of LQ to fermions to zero. Furthermore, here we give the results solely for the phenomenologically interesting representations, Φ_3, V_1^μ and V_3^μ. Only they give a good fit to $b\to s\ell^+\ell^-$ data as they generate left-handed currents. The complete tree-level matching (including right-handed couplings) for all LQ representations and all semileptonic B decays and $\ell\to\ell'\gamma$ processes can be found in the Appendix.

Starting with $b\to s\ell^+\ell^-$ transitions we use the effective Hamiltonian,

$$\mathcal{H}^{\ell_f\ell_i}_{\rm eff} = -\frac{4G_F}{\sqrt{2}}V_{tb}V^*_{ts}\sum_k C^{fi}_k O^{fi}_k + \text{H.c.} \tag{7}$$

restricted to operators with left-handed couplings:

$$\begin{aligned}O^{fi}_9 &= \frac{\alpha}{4\pi}\bar{s}\gamma_\mu P_L b\bar{\ell}_f\gamma^\mu\ell_i,\\ O^{fi}_{10} &= \frac{\alpha}{4\pi}\bar{s}\gamma_\mu P_L b\bar{\ell}_f\gamma^\mu\gamma_5\ell_i.\end{aligned} \tag{8}$$

The Wilson coefficients $C^{fi}_{9(10)}$ can then be expressed as

$$\begin{aligned}\Phi_3\colon\ C^{fi}_9 &= -C^{fi}_{10} = +\lambda^3_{3i}\lambda^{3*}_{2f}\frac{\sqrt{2}}{2G_F V_{tb}V^*_{ts}}\frac{\pi}{\alpha}\frac{1}{M^2},\\ V_1^\mu\colon\ C^{fi}_9 &= -C^{fi}_{10} = -\kappa^{1L}_{2i}\kappa^{1L*}_{3f}\frac{\sqrt{2}}{2G_F V_{tb}V^*_{ts}}\frac{\pi}{\alpha}\frac{1}{M^2},\\ V_3^\mu\colon\ C^{fi}_9 &= -C^{fi}_{10} = -\kappa^{3}_{2i}\kappa^{3*}_{3f}\frac{\sqrt{2}}{2G_F V_{tb}V^*_{ts}}\frac{\pi}{\alpha}\frac{1}{M^2}\end{aligned} \tag{9}$$

with the leptoquark mass M. The complete results for the Wilson coefficients originating for the 10 representations of scalar and vector LQ are given in the Appendix. In order to constrain the Wilson coefficients $C^{ee,\mu\mu}_{9(10)}$ we use the global fit of Ref. [5] to $b\to s\ell^+\ell^-$ data.

For the $b\to s\mu e$ transitions we use the results of Ref. [44]:

$$\begin{aligned}&\text{Br}[B_s\to\mu^+e^-]\\ &\quad=\frac{\tau_{B_s}m_\mu^2 M_{B_s}f^2_{B_s}}{64\pi^3}\alpha^2G_F^2|V_{tb}V^*_{ts}|^2\left(1-\frac{m_\mu^2}{M^2_{B_s}}\right)^2\\ &\qquad\times(|C^{\mu e}_9|^2+|C^{\mu e}_{10}|^2),\end{aligned} \tag{10}$$

$$\begin{aligned}&\text{Br}[B\to K^{(*)}\mu^+e^-]\\ &\quad=10^{-9}(a_{K^{(*)}}|C^{\mu e}_9|^2+b_{K^{(*)}}|C^{\mu e}_{10}|^2+c_{K^{(*)}}|C^{e\mu}_9|^2\\ &\qquad+d_{K^{(*)}}|C^{\mu e}_{10}|^2),\end{aligned} \tag{11}$$

with

$$\begin{aligned}&a_K=15.4\pm3.1,\qquad b_K=15.7\pm3.1,\\ &c_K=0,\qquad d_K=0,\\ &a_{K^*}=5.6\pm1.9,\qquad b_{K^*}=5.6\pm1.9,\\ &c_{K^*}=29.1\pm4.9,\qquad d_{K^*}=29.1\pm4.9.\end{aligned} \tag{12}$$

Note that these results are for μ^+e^- final states and not for the sums $\mu^\pm e^\mp=\mu^-e^++\mu^+e^-$ that are constrained experimentally [41].

Let us now consider the lepton flavor violating processes $\mu\to e\gamma$. Evaluating the loop diagrams depicted in Fig. 1 for the three leptoquark representations in which we are interested, we find the branching ratios

$$\text{Br}[\mu\to e\gamma] = \tau_\mu\frac{\alpha m_\mu^3}{256\pi^4}|C^{e\mu}_L|^2 \tag{13}$$

with

$$\begin{aligned}\Phi_3\colon\ C^{e\mu}_L &= -N_c\frac{\lambda^{3*}_{j1}\lambda^3_{j2}m_\mu}{8M^2},\\ V_1^\mu\colon\ C^{e\mu}_L &= +N_c\frac{\kappa^{1L*}_{j1}\kappa^{1L}_{j2}m_\mu}{6M^2},\\ V_3^\mu\colon\ C^{e\mu}_L &= +N_c\frac{2\kappa^{3*}_{j1}\kappa^{3}_{j2}m_\mu}{M^2}.\end{aligned} \tag{14}$$

The complete formula for all leptoquarks is given in the Appendix. Here we did not follow the approach of Ref. [45] but rather calculated the effect in unitary gauge which gives a UV finite result. Note that this is possible since the remaining Higgs sector (or additional composite dynamics) can be decoupled such that it does not affect $\mu\to e\gamma$.

In general, LQ can also account for the anomalous magnetic moment (AMM) of the muon [19,24,29–32, 45–50]. However, this would require chirally enhanced effects which also enhance $\ell\to\ell'\gamma$ processes. This enhancement is so large, that $\mu\to e\gamma$ would rule out any effect in electrons in $b\to s\ell^+\ell^-$ transitions if one accounted for the AMM of the muon [32]. Therefore, we will assume the absence of chiral enhancement in our phenomenological analysis and assume that the LQ couple only to left-handed fermions.

In principle also contributions to $\mu \to 3e$ arise at the one-loop level in LQ models with couplings to μ and e. While the box contributions are suppressed by four small LQ-quark-lepton couplings (as estimated from the $b \to s\ell^+\ell^-$ anomalies) Z penguins are potentially important. They can lead to branching ratios of the order of 10^{-15} which is interesting in the light of the future expected sensitivity [51]. This is due to the contribution of internal top quarks leading to an enhancement m_t^2/m_Z^2. However, the same Z penguin also generates effects in $\mu \to e$ conversion. In this case also tree-level effects can arise, depending on the couplings to the first generation of quarks. We postpone a detailed analysis of these effects to a forthcoming publication.

LQ also contribute to $b \to s\bar{\nu}\nu$ and $b \to c\ell\bar{\nu}$ transitions. For muons and electrons, these processes do not give relevant constraints. However, they are in general important once tau leptons are involved and the corresponding formulas are given in the Appendix.

III. PHENOMENOLOGICAL ANALYSIS

As stated above, we focus on the three LQ representations that can give a good fit to $b \to s\mu^+\mu^-$ data for the phenomenological analysis: Φ_3, V_1^μ, and V_3^μ. In addition, we assume that the couplings to right-handed fermions vanish such that all three representations give a pure $C_9 = -C_{10}$-like contribution. Furthermore, we neglect the couplings of the LQ to the first generation of quarks. If one takes the deviations from the SM predictions in $b \to c\tau\nu$ processes seriously, the mass scale of the LQ should be around 2 TeV for perturbative couplings. However, $b \to s\ell^+\ell^-$ data can also be explained for much heavier LQs (above 10 TeV) if the couplings are sizable.

Once the LQ couple to muons and electrons simultaneously, we get correlated effects in $\mu \to e\gamma$, $B_s \to \mu e$ and $B \to K^{(*)}\mu e$. Combining (9) and (14) with (11) and (13), we can express the lepton flavor violating branching ratios in terms of the Wilson coefficients $C_9^{\mu\mu}$ and C_9^{ee} as

$$\mathrm{Br}[\mu \to e\gamma] = \tau_\mu \frac{\alpha^3 G_F^2 m_\mu^5}{512\pi^6} |V_{tb}V_{ts}^*|^2 N_c^2 \left(\chi C_9^{ee} + \frac{C_9^{\mu\mu}}{\chi}\right)^2 \times \begin{cases} 1/16 & \Phi_3 \\ 1/9 & V_1^\mu \\ 16 & V_3^\mu \end{cases}, \tag{15}$$

$$\mathrm{Br}[B \to K\mu^\pm e^\mp] = 10^{-9}(a_K + b_K)\left[\left(\frac{C_9^{ee}}{\gamma}\right)^2 + (\gamma C_9^{\mu\mu})^2\right]. \tag{16}$$

Here we defined the ratios $\chi = y_{32}/y_{21}$ and $\gamma = y_{21}/y_{22}$, with $y = \lambda$ for scalar LQ and $y = \kappa$ for vector LQ.

Note that the constraints from $\mu \to e\gamma$ on the scalar LQ triplet is weakest, resulting in the biggest allowed region in parameter space and that the effect in $b \to s\mu e$ transitions does not depend on the specific representation. Our results are shown in Fig. 2 for various values of χ and γ. Interestingly, for real couplings, there is a cancellation in the contributions to $\mu \to e\gamma$ if $\mathrm{sgn}C_9^{\mu\mu} = -\mathrm{sgn}C_9^{ee}$. This means that if, in the future, the global fit required equal signs for $C_9^{\mu\mu}$ and C_9^{ee}, a LQ explanation (with real couplings) of the anomalies would be ruled out. Furthermore, the predicted rates for $B_s \to \mu e$, $B \to K\mu e$ and $B \to K^*\mu e$ are within the reach of LHCb and BELLE II. In Fig. 2, we only showed $B \to K\mu e$ for which the predicted rate is closest to the current experimental limit. For the other processes, we have

$$\mathrm{Br}[B \to K^*\mu e]/\mathrm{Br}[B \to K\mu e] \approx 2.2, \quad \mathrm{Br}[B_s \to \mu e]/\mathrm{Br}[B \to K\mu e] \approx 0.006 \tag{17}$$

in our $C_9 = -C_{10}$ setup.

IV. τ-μ AND τ-e TRANSITIONS

Once one allows for couplings of leptoquarks to tau leptons as well, τ-μ and τ-e transitions are also generated. The corresponding processes are experimentally much less constrained than μ-e transitions. In fact, the most constraining processes involving tau flavors are $B \to K^{(*)}\bar{\nu}\nu$ which include tau neutrinos. In order to generate measurable effects in processes with charged tau leptons, the corresponding effect in neutrinos must be absent or suppressed. The only single LQ representation which gives a good fit to $b \to s\mu^+\mu^-$ data and does not generate effects in $b \to s\bar{\nu}\nu$ is the vector singlet V_1^μ. However, this LQ has the same tree-level phenomenology as the combination of a scalar singlet and a scalar triplet studied in Ref. [15]. Furthermore, since in the absence of right-handed couplings $\tau \to \mu\gamma$ and $\tau \to e\gamma$ are not important, we refer the reader to Ref. [15] where the interplay between $b \to s\tau\mu$, $b \to s\bar{\nu}\nu$ and $b \to s\mu^+\mu^-$ processes is shown.

V. CONCLUSIONS AND OUTLOOK

In this article, we have studied the possibility that LQ contribute to $b \to s\mu^+\mu^-$ and $b \to se^+e^-$ processes simultaneously in order to explain the hints for LFU violation in $R(K)$ and $R(K^*)$, generating lepton flavor violation as well. We calculated the tree-level matching for semileptonic B decays for all ten (five scalar and five vector) LQ representations and their effects at one loop in $\ell \to \ell'\gamma$.

In our phenomenological analysis, we considered the three LQ representations (Φ_3, V_1^μ and V_3^μ) giving a good fit to $b \to s\ell^+\ell^-$ data. In this setup, we found an interesting interplay between $b \to s\ell^+\ell^-$, $\mu \to e\gamma$ and $b \to s\mu e$ processes, showing that the current constraints are within the same ballpark. The amount of tuning between the electron and the muon coupling of the LQ required by $\mu \to e\gamma$ depends on representation chosen as well as on the ratio χ. In general, the effect of the Φ_3 in $\mu \to e\gamma$ is smallest and therefore less tuning is required than for the other LQs. Interestingly, if forthcoming data requires NP contributions to electron and muon channels simultaneously, there are also very good prospects of discovering nonzero decay rates for processes like $B_s \to \mu e$ or $\mu \to e\gamma$ with measurements in the near future. Furthermore, (for real couplings) one could rule out a LQ explanation $b \to s\ell^+\ell^-$ if $C_9^{\mu\mu}$ has the same sign as C_9^{ee} since this is in conflict with $\mu \to e\gamma$ bounds.

ACKNOWLEDGMENTS

The work of A. C. and D. M. is supported by an Ambizione Grant of the Swiss National Science Foundation (PZ00P2_154834). Y. U. is supported by the Swiss National Science Foundation (SNF) under Contract No. 200021_163466. We are grateful to Bernat Capdevila and Joaquim Matias for providing us the fit to $b \to s\ell^+\ell^-$ for the scenario $C_9^{\mu\mu} = -C_{10}^{\mu\mu}$ and $C_9^{ee} = -C_{10}^{ee}$. We thank Toshihiko Ota and Giovanni Marco Pruna for checking the sign of the Wilson coefficients originating from the tree-level matching. We also thank Giovanni Marco Pruna for useful discussions and pointing out the consistency of the calculation of $\mu \to e\gamma$ in the unitary gauge.

APPENDIX: MATCHING

In this appendix, we present the tree-level matching for semileptonic $b \to s$ and $b \to c$ processes and the loop effect in $\ell \to \ell'\gamma$ for all ten leptoquark representations. Contrary to the results presented in the main article, we keep right-handed couplings.

In order to simplify the calculation, one can write interactions of LQ with quarks and leptons completely generic in the following form,

$$\begin{aligned} &\bar{q}_f^{(c)}(\Gamma_{fi}^R P_R + \Gamma_{fi}^L P_L)\ell_i^{(c)}\Phi_A^*, \\ &\bar{q}_f^{(c)}(\Gamma_{fi}^{VR}\gamma_\mu P_R + \Gamma_{fi}^{VL}\gamma_\mu P_L)\ell_i^{(c)}V_A^{\mu*}, \end{aligned} \tag{A1}$$

with

$$\begin{aligned} &\Phi_A \in \{\Phi_1, \tilde{\Phi}_1, \Phi_2, \tilde{\Phi}_2, \Phi_3\}, \\ &V_A^\mu \in \{V_1^\mu, \tilde{V}_1^\mu, V_2^\mu, \tilde{V}_2^\mu, V_3^\mu\}, \end{aligned} \tag{A2}$$

the scalar and vector LQ, respectively. The superscript (c) denotes a possible charge conjugation of the field. The explicit form of the couplings $\Gamma_{fi}^{R,L}$ and $\Gamma_{fi}^{VR,VL}$ for the various representations is given in Table I. Here, we chose to work in the down basis, i.e. CKM rotations appear in the couplings once interactions with left-handed up quarks are present. All other rotations necessary to go from the interaction to the mass eigenbasis are unphysical and can be absorbed into a redefinition of the couplings.

TABLE I. Couplings for the different representations of scalar and vector LQ to quarks and leptons.

	Representation	Γ_{fi}^R	Γ_{fi}^L
$\bar{u}_f\ell_i$	Φ_2	$V_{fj}\lambda_{ji}^{2LR}$	λ_{fi}^{2RL}
$\bar{u}_f\nu_i$	Φ_2	0	λ_{fi}^{2RL}
$\bar{d}_f\ell_i$	Φ_2	$-\lambda_{fi}^{2LR}$	0
	$\tilde{\Phi}_2$	0	$\tilde{\lambda}_{fi}^2$
$\bar{d}_f\nu_i$	$\tilde{\Phi}_2$	0	$\tilde{\lambda}_{fi}^2$
$\bar{u}_f^c\ell_i$	Φ_1	λ_{fi}^{1R}	$V_{fj}^*\lambda_{ji}^{1L}$
	Φ_3	0	$-V_{fj}^*\lambda_{ji}^3$
$\bar{u}_f^c\nu_i$	Φ_3	0	$\sqrt{2}V_{fj}^*\lambda_{jf}^3$
$\bar{d}_f^c\ell_f$	$\tilde{\Phi}_1$	$\tilde{\lambda}_{fi}^1$	0
	Φ_3	0	$-\sqrt{2}\lambda_{fi}^3$
$\bar{d}_f^c\nu_i$	Φ_1	0	$-\lambda_{fi}^{1L}$
	Φ_3	0	$-\lambda_{fi}^3$

	Representation	Γ_{fi}^{VR}	Γ_{fi}^{VL}
$\bar{u}_f\ell_i$	$\tilde{V}_1^\mu$	$\tilde{\kappa}_{fi}^1$	0
	V_3^μ	0	$\sqrt{2}V_{fj}\kappa_{ji}^3$
$\bar{u}_f\nu_i$	V_1^μ	0	$\kappa_{ji}^{1L}V_{jf}$
	V_3^μ	0	$V_{fj}\kappa_{ji}^3$
$\bar{d}_f\ell_i$	V_1^μ	κ_{fi}^{1R}	κ_{fi}^{1L}
	V_3^μ	0	$-\kappa_{fi}^3$
$\bar{d}_f\nu_i$	V_3^μ	0	$\sqrt{2}\kappa_{fi}^3$
$\bar{u}_f^c\ell_i$	V_2^μ	$V_{fj}^*\kappa_{ji}^{2LR}$	0
	$\tilde{V}_2^\mu$	0	$\tilde{\kappa}_{fi}^2$
$\bar{u}_f^c\nu_i$	$\tilde{V}_2^\mu$	0	$\tilde{\kappa}_{fi}^2$
$\bar{d}_f^c\ell_i$	V_2^μ	κ_{fi}^{2LR}	κ_{fi}^{2RL}
$\bar{d}_f^c\nu_i$	V_2^μ	0	κ_{fi}^{2RL}

1. $b \to s\ell^+\ell^-$

For $b \to s\ell^+\ell^-$ transitions, we use the effective Hamiltonian in Eq. (7), also including operators with right-handed couplings,

$$\begin{aligned} O_9^{(\prime)fi} &= \frac{\alpha}{4\pi}\bar{s}\gamma_\mu P_{L(R)}b\bar{\ell}_f\gamma^\mu\ell_i, \\ O_{10}^{(\prime)fi} &= \frac{\alpha}{4\pi}\bar{s}\gamma_\mu P_{L(R)}b\bar{\ell}_f\gamma^\mu\gamma_5\ell_i, \end{aligned} \tag{A3}$$

$$\begin{aligned} O_S^{(\prime)fi} &= \frac{\alpha}{4\pi}\bar{s}P_{L(R)}b\bar{\ell}_f\ell_i, \\ O_P^{(\prime)fi} &= \frac{\alpha}{4\pi}\bar{s}P_{L(R)}b\bar{\ell}_f\gamma_5\ell_i. \end{aligned} \tag{A4}$$

The Wilson coefficients originating for the ten representations of scalar and vector LQ are given in Table II. Each entry should be understood to be multiplied by a factor

TABLE II. Contribution of the ten LQ representations to $b \to s\ell_i^+\ell_f^-$. Each entry should be multiplied by $\frac{\sqrt{2}}{4G_F V_{tb}V_{ts}^*}\frac{\pi}{\alpha}\frac{1}{M^2}$.

$b \to s\ell_i^+\ell_f^-$	C_9^{fi}	C_{10}^{fi}	$C_9^{\prime fi}$	$C_{10}^{\prime fi}$	$C_S^{fi} = C_P^{fi}$	$C_S^{\prime fi} = -C_P^{\prime fi}$
Φ_1	0	0	0	0	0	0
Φ_3	$2\lambda_{3i}^3\lambda_{2f}^{3*}$	$-2\lambda_{3i}^3\lambda_{2f}^{3*}$	0	0	0	0
Φ_2	$-\lambda_{2i}^{2LR}\lambda_{3f}^{2LR*}$	$-\lambda_{2i}^{2LR}\lambda_{3f}^{2LR*}$	0	0	0	0
$\tilde{\Phi}_2$	0	0	$-\tilde{\lambda}_{2i}^2\tilde{\lambda}_{3f}^{2*}$	$\tilde{\lambda}_{2i}^2\tilde{\lambda}_{3f}^{2*}$	0	0
$\tilde{\Phi}_1$	0	0	$\tilde{\lambda}_{3i}^1\tilde{\lambda}_{2f}^{1*}$	$\tilde{\lambda}_{3i}^1\tilde{\lambda}_{2f}^{1*}$	0	0
V_1^μ	$-2\kappa_{2i}^{1L}\kappa_{3f}^{1L*}$	$2\kappa_{2i}^{1L}\kappa_{3f}^{1L*}$	$-2\kappa_{2i}^{1R}\kappa_{3f}^{1R*}$	$-2\kappa_{2i}^{1R}\kappa_{3f}^{1R*}$	$4\kappa_{2i}^{1L}\kappa_{3f}^{1R*}$	$4\kappa_{2i}^{1L}\kappa_{3f}^{1R*}$
V_3^μ	$-2\kappa_{2i}^3\kappa_{3f}^{3*}$	$2\kappa_{2i}^3\kappa_{3f}^{3*}$	0	0	0	0
V_2^μ	$2\kappa_{3i}^{2RL}\kappa_{2f}^{2RL*}$	$2\kappa_{3i}^{2RL}\kappa_{2f}^{2RL*}$	$2\kappa_{3i}^{2LR}\kappa_{2f}^{2LR*}$	$-2\kappa_{3i}^{2LR}\kappa_{2f}^{2LR*}$	$4\kappa_{3i}^{2LR}\kappa_{2f}^{2RL*}$	$4\kappa_{3i}^{2LR}\kappa_{2f}^{2RL*}$
$\tilde{V}_1^\mu$	0	0	0	0	0	0
$\tilde{V}_2^\mu$	0	0	0	0	0	0

$$\frac{\sqrt{2}}{4G_F V_{tb}V_{ts}^*}\frac{\pi}{\alpha}\frac{1}{M^2}. \tag{A5}$$

For $i \neq f$, we also get contributions to lepton flavor violating B decays.

$$\begin{aligned}\mathrm{Br}[B_s \to \ell^+\ell'^-] = \frac{\tau_{B_s}\mathrm{Max}[m_\ell^2, m_{\ell'}^2]M_{B_s}f_{B_s}^2}{64\pi^3}\alpha^2 G_F^2|V_{tb}V_{ts}^*|^2\left(1-\frac{\mathrm{Max}[m_\ell^2, m_{\ell'}^2]}{M_{B_s}^2}\right)^2 \\ \times(|C_9^{\ell\ell'} - C_9^{\prime\ell\ell'}|^2 + |C_{10}^{\ell\ell'} - C_{10}^{\prime\ell\ell'}|^2),\end{aligned} \tag{A6}$$

$$\begin{aligned}\mathrm{Br}[B \to K^{(*)}\ell^+\ell'^-] = 10^{-9}(a_{K^{(*)}\ell\ell'}|C_9^{\ell\ell'} + C_9^{\prime\ell\ell'}|^2 + b_{K^{(*)}\ell\ell'}|C_{10}^{\ell\ell'} + C_{10}^{\prime\ell\ell'}|^2 \\ + c_{K^{(*)}\ell\ell'}|C_9^{\ell\ell'} - C_9^{\prime\ell\ell'}|^2 + d_{K^{(*)}\ell\ell'}|C_{10}^{\ell\ell'} - C_{10}^{\prime\ell\ell'}|^2),\end{aligned} \tag{A7}$$

with

$\ell\ell'$	$a_{K\ell\ell'}$	$b_{K\ell\ell'}$	$c_{K\ell\ell'}$	$d_{K\ell\ell'}$	$a_{K^*\ell\ell'}$	$b_{K^*\ell\ell'}$	$c_{K^*\ell\ell'}$	$d_{K^*\ell\ell'}$
$\tau\mu/\tau e$	9.6 ± 1.0	10.0 ± 1.3	0	0	3.0 ± 0.8	2.7 ± 0.7	16.4 ± 2.1	15.4 ± 1.9
μe	15.4 ± 3.1	15.7 ± 3.1	0	0	5.6 ± 1.9	5.6 ± 1.9	29.1 ± 4.9	29.1 ± 4.9

Note that the results in (A6) and (A7) are for $\ell^-\ell'^+$ final states and not for the sums $\ell^\pm\ell'^\mp = \ell^-\ell'^+ + \ell^+\ell'^-$ constrained experimentally.

2. $b \to s\bar{\nu}\nu$

Here, we match the Wilson coefficients on the effective Hamiltonian defined as

$$\mathcal{H}_{\mathrm{eff}}^{\nu_f\nu_i} = -\frac{4G_F}{\sqrt{2}}V_{tb}V_{ts}^*\sum_k C_k^{fi}O_k^{fi} + \mathrm{H.c.} \tag{A8}$$

with the operators given by

$$O_{L(R)}^{fi} = \frac{\alpha}{4\pi}\bar{s}\gamma_\mu P_{L(R)}b\bar{\nu}_f\gamma^\mu(1-\gamma_5)\nu_i. \tag{A9}$$

The results for the corresponding Wilson coefficients are given in Table III, where the overall factor

$$\frac{\sqrt{2}}{4G_F V_{tb}V_{ts}^*}\frac{\pi}{\alpha}\frac{1}{M^2} \tag{A10}$$

is omitted. The ratios between the measurements of $B \to K^{(*)}\bar{\nu}\nu$ and the SM

TABLE III. Contribution of the various LQ representations to $b\to s\bar\nu_i\nu_f$. Each entry should be multiplied by a factor $\frac{\sqrt{2}}{4G_F V_{tb}V_{ts}^*}\frac{\pi}{\alpha}\frac{1}{M^2}$.

$b\to s\bar\nu_i\nu_f$	C_L^{fi}	C_R^{fi}
Φ_1	$\lambda_{3i}^{1L}\lambda_{2f}^{1L*}$	0
Φ_3	$\lambda_{3i}^{3}\lambda_{2f}^{3*}$	0
Φ_2	0	0
$\tilde\Phi_2$	0	$-\tilde\lambda_{2i}^{2}\tilde\lambda_{3f}^{2*}$
$\tilde\Phi_1$	0	0
V_1^μ	0	0
V_3^μ	$-4\kappa_{2i}^{3}\kappa_{3f}^{3*}$	0
V_2^μ	0	$2\kappa_{3i}^{2LR}\kappa_{2f}^{LR*}$
$\tilde V_1^\mu$	0	0
$\tilde V_2^\mu$	0	0

$$\mathcal{R}_{K^{(*)}} = \frac{\mathrm{Br}[B\to K^{(*)}\bar\nu\nu]}{\mathrm{Br}[B\to K^{(*)}\bar\nu\nu]_{\mathrm{SM}}} \gg 1 \tag{A11}$$

are currently much larger than one.

3. $b\to c\ell\bar\nu$

For completeness, we also consider the charged current effective Hamiltonian,

TABLE IV. Contribution of the various LQ representation to $b\to c\bar\nu_i\ell_f^-$. Each entry should be multiplied by a factor $\frac{-\sqrt{2}}{8G_F V_{cb}}\frac{1}{M^2}$.

$b\to c\bar\nu_i\ell_f^-$	C_{VL}^{fi}	C_{VR}^{fi}	C_{SL}^{fi}	C_{SR}^{fi}	C_{TL}^{fi}
Φ_1	$-\lambda_{3i}^{1L}V_{2j}\lambda_{jf}^{1L*}$	0	$\lambda_{3i}^{1L}\lambda_{2f}^{1R*}$	0	$-\frac{1}{4}\lambda_{3i}^{1L}\lambda_{2f}^{1R*}$
Φ_3	$\lambda_{3i}^{3}V_{2j}\lambda_{jf}^{3*}$	0	0	0	0
Φ_2	0	0	$\lambda_{2i}^{2RL}\lambda_{3f}^{2LR*}$	0	$\frac{1}{4}\lambda_{2i}^{2RL}\lambda_{3f}^{2LR*}$
$\tilde\Phi_2$	0	0	0	0	0
$\tilde\Phi_1$	0	0	0	0	0
V_1^μ	$-2\kappa_{3f}^{1L*}V_{2j}\kappa_{ji}^{1L}$	0	0	$4\kappa_{3f}^{1R*}V_{2j}\kappa_{ji}^{1L}$	0
V_3^μ	$2\kappa_{3f}^{3*}V_{2j}\kappa_{ji}^{3}$	0	0	0	0
V_2^μ	0	0	0	$4\kappa_{3i}^{2RL}V_{2j}\kappa_{jf}^{2LR*}$	0
$\tilde V_1^\mu$	0	0	0	0	0
$\tilde V_2^\mu$	0	0	0	0	0

$$\mathcal{H}_{\mathrm{eff}}^{\ell_f\nu_i} = \frac{4G_F}{\sqrt{2}}V_{cb}\sum_k C_k^{fi}O_k^{fi} + \mathrm{H.c.}, \tag{A12}$$

with

$$\begin{aligned} O_{VL(R)}^{fi} &= \bar c\gamma^\mu P_{L(R)}b\bar\ell_f\gamma_\mu P_L\nu_i,\\ O_{SL(R)}^{fi} &= \bar c P_{L(R)}b\bar\ell_f P_L\nu_i,\\ O_{TL}^{fi} &= \bar c\sigma^{\mu\nu}P_L b\bar\ell_f\sigma_{\mu\nu}P_L\nu_i. \end{aligned} \tag{A13}$$

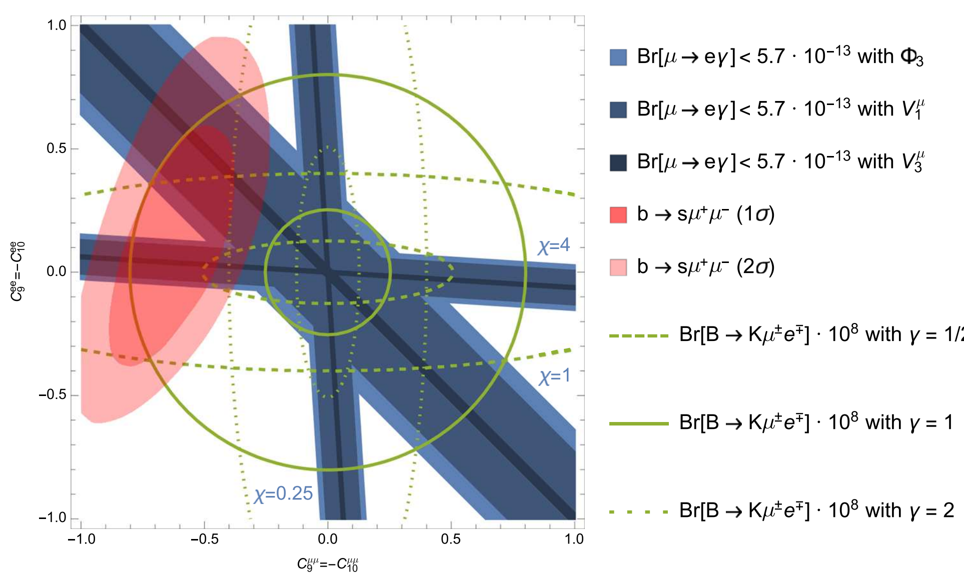

FIG. 2. Regions allowed by MEG (shades of blue) and $b\to s\mu^+\mu^-$ (red) in the $C_9^{\mu\mu}$–C_9^{ee} plane [52] with $C_9=-C_{10}$. The different representations are color-coded in the darkness of the different blues: the light-blue region corresponds to Φ_3, the medium one to V_1^μ and the dark blue region to V_3^μ. The bands rotated relative to the $\chi=1$ region show the situation for $\chi=4$ and $\chi=1/4$, respectively. The green contours represent the branching ratio $B\to K\mu^\pm e^\mp$ with $\gamma=1$ (solid line), $\gamma=1/2$ (dashed) and $\gamma=2$ (dotted). In each case, the inner line describes $\mathrm{Br}[B\to K\mu^\pm e^\mp]=0.2\times10^{-8}$ and the outer one $\mathrm{Br}[B\to K\mu^\pm e^\mp]=2\times10^{-8}$. Note that these contours do not depend on the specific LQ representation.

TABLE V. Contribution of the ten LQ representations to $\ell_i \to \ell_f\gamma$ assuming $m_{\ell_f} = 0$. An additional factor N_c is understood. For the scalar LQ doublets the Wilson coefficients with down-type quarks vanish because of the factor $1 + 3Q_d$.

$\ell_i \to \ell_f\gamma$	C_L^{fi}	C_R^{fi}
Φ_1	$\frac{\lambda_{jf}^{1L*}\lambda_{ji}^{1L}m_{\ell_i}}{24M^2} - \frac{\lambda_{jf}^{1R*}V_{jk}^{*}\lambda_{ki}^{1L}m_{u_j}(7+4\log(y_{u_j}))}{12M^2}$	$\frac{\lambda_{jf}^{1R*}\lambda_{ji}^{1R}m_{\ell_i}}{24M^2} - \frac{V_{jk}\lambda_{kf}^{1L*}\lambda_{ji}^{1R}m_{u_j}(7+4\log(y_{u_j}))}{12M^2}$
$\tilde{\Phi}_1$	0	$-\frac{\tilde{\lambda}_{jf}^{1*}\tilde{\lambda}_{ji}^{1}m_{\ell_i}}{12M^2}$
Φ_2	$-\frac{\lambda_{jf}^{2RL*}\lambda_{ji}^{2RL}m_{\ell_i}}{8M^2} + \frac{\lambda_{jf}^{2RL*}V_{jk}\lambda_{ki}^{2LR}m_{u_j}(1+4\log(y_{u_j}))}{12M^2}$	$-\frac{\lambda_{jf}^{2LR*}\lambda_{ji}^{2LR}m_{\ell_i}}{8M^2} + \frac{V_{jk}^{*}\lambda_{kf}^{2LR*}\lambda_{ji}^{2RL}m_{u_j}(1+4\log(y_{u_j}))}{12M^2}$
$\tilde{\Phi}_2$	0	0
Φ_3	$-\frac{\lambda_{jf}^{3*}\lambda_{ji}^{3}m_{\ell_i}}{8M^2}$	0
V_1^μ	$\frac{\kappa_{jf}^{1L*}\kappa_{ji}^{1L}m_{\ell_i}}{6M^2} - \frac{\kappa_{jf}^{1R}\kappa_{ji}^{1L}m_{d_j}}{3M^2}$	$\frac{\kappa_{jf}^{1R*}\kappa_{ji}^{1R}m_{\ell_i}}{6M^2} - \frac{\kappa_{jf}^{1L*}\kappa_{ji}^{1R}m_{d_j}}{M^2}$
$\tilde{V}_1^\mu$	0	$\frac{11\tilde{\kappa}_{jf}^{1*}\tilde{\kappa}_{ji}^{1}m_{\ell_i}}{12M^2}$
V_2^μ	$\frac{2\kappa_{jf}^{2RL*}\kappa_{ji}^{2RL}m_{\ell_i}}{3M^2} - \frac{5\kappa_{jf}^{2LR*}\kappa_{ji}^{2RL}m_{d_j}}{3M^2}$	$\frac{7\kappa_{jf}^{2LR*}\kappa_{ji}^{2LR}m_{\ell_i}}{12M^2} - \frac{5\kappa_{jf}^{2RL*}\kappa_{ji}^{2LR}m_{d_j}}{3M^2}$
$\tilde{V}_2^\mu$	$-\frac{\tilde{\kappa}_{jf}^{2*}\kappa_{ji}^{2}m_{\ell_i}}{12M^2}$	0
V_3^μ	$\frac{2\kappa_{jf}^{3*}\kappa_{ji}^{3}m_{\ell_i}}{M^2}$	0

The Wilson coefficients expressed in terms of the LQ couplings are given in Table IV, with an overall factor

$$\frac{-\sqrt{2}}{8G_F V_{cb}}\frac{1}{M^2} \tag{A14}$$

omitted.

Considering only couplings to muons and electrons, the effects in $B \to D^{(*)}\ell\nu$ are below the percent level once the constraints from $b \to s\ell^+\ell^-$ are taken into account and therefore phenomenologically not relevant.

4. $\ell_i \to \ell_f\gamma$

Here the branching ratios are given by

$$\mathrm{Br}[\ell_i \to \ell_f\gamma] = \tau_{\ell_i}\frac{\alpha m_{\ell_i}^3}{256\pi^4}(|C_L^{fi}|^2 + |C_R^{fi}|^2). \tag{A15}$$

Working with a generic charge Q for the quark propagating in the loop, we obtain for a vector LQ,

$$C_L^{fi} = N_c\left(\frac{\Gamma_{jf}^{VL*}\Gamma_{ji}^{VL}m_{\ell_i}(5+9Q)}{12M^2} - \frac{\Gamma_{jf}^{VR*}\Gamma_{ji}^{VL}m_{q_j}(1+2Q)}{M^2}\right), \tag{A16}$$

and for a scalar LQ

$$C_L^{fi} = N_c\left(-\frac{\Gamma_{jf}^{L*}\Gamma_{ji}^{L}m_{\ell_i}(1+3Q)}{24M^2} + \frac{\Gamma_{jf}^{L*}\Gamma_{ji}^{R}m_{q_j}(-1+2Q+2Q\log(y_{q_j}))}{4M^2}\right), \tag{A17}$$

where $y_{q_j} = m_{q_j}^2/M^2$ and C_R is obtained from C_L by exchanging L with R. The explicit expressions for C_L^{fi} and C_R^{fi} for the various representations after summing over the $SU(2)$ components are given in Table V.

[1] W. Altmannshofer and D. M. Straub, *Proceedings, 50th Rencontres de Moriond Electroweak Interactions and Unified Theories: La Thuile, Italy, March 14-21* (2015) pp. 333–338.
[2] S. Descotes-Genon, L. Hofer, J. Matias, and J. Virto, J. High Energy Phys. 06 (2016) 092.
[3] T. Hurth, F. Mahmoudi, and S. Neshatpour, Nucl. Phys. **B909**, 737 (2016).
[4] R. Aaij *et al.* (LHCb), J. High Energy Phys. 08 (2017) 055.
[5] B. Capdevila, A. Crivellin, S. Descotes-Genon, J. Matias, and J. Virto, arXiv:1704.05340.
[6] Y. Amhis *et al.*, arXiv:1612.07233.
[7] B. Gripaios, M. Nardecchia, and S. Renner, J. High Energy Phys. 05 (2015) 006.
[8] S. Fajfer and N. Košnik, Phys. Lett. B **755**, 270 (2016).
[9] D. Becirevic, S. Fajfer, and N. Kosnik, arXiv:1503.09024.
[10] I. d. M. Varzielas and G. Hiller, J. High Energy Phys. 06 (2015) 072.
[11] R. Alonso, B. Grinstein, and J. M. Camalich, J. High Energy Phys. 10 (2015) 184.
[12] L. Calibbi, A. Crivellin, and T. Ota, Phys. Rev. Lett. **115**, 181801 (2015).
[13] R. Barbieri, G. Isidori, A. Pattori, and F. Senia, Eur. Phys. J. C **76**, 67 (2016).
[14] D. Becirevic, N. Kosnik, O. Sumensari, and R. Zukanovich Funchal, J. High Energy Phys. 11 (2016) 035.
[15] A. Crivellin, D. Mueller, and T. Ota, J. High Energy Phys. 09 (2017) 040.
[16] D. Bečirević and O. Sumensari, J. High Energy Phys. 08 (2017) 104.
[17] Y. Cai, J. Gargalionis, M. A. Schmidt, and R. R. Volkas, J. High Energy Phys. 10 (2017) 047.
[18] S. Fajfer, J. F. Kamenik, I. Nisandzic, and J. Zupan, Phys. Rev. Lett. **109**, 161801 (2012).
[19] M. Bauer and M. Neubert, Phys. Rev. Lett. **116**, 141802 (2016).
[20] X.-Q. Li, Y.-D. Yang, and X. Zhang, J. High Energy Phys. 08 (2016) 054.
[21] D. Bečirević, S. Fajfer, N. Košnik, and O. Sumensari, Phys. Rev. D **94**, 115021 (2016).
[22] S. Sahoo, R. Mohanta, and A. K. Giri, Phys. Rev. D **95**, 035027 (2017).
[23] R. Barbieri, C. W. Murphy, and F. Senia, Eur. Phys. J. C **77**, 8 (2017).
[24] C.-H. Chen, T. Nomura, and H. Okada, Phys. Lett. B **774**, 456 (2017).
[25] W. Altmannshofer, P. S. B. Dev, and A. Soni, Phys. Rev. D **96**, 095010 (2017).
[26] I. Doršner, S. Fajfer, D. A. Faroughy, and N. Košnik, J. High Energy Phys. 10 (2017) 188.
[27] F. Feruglio, P. Paradisi, and A. Pattori, J. High Energy Phys. 09 (2017) 061.
[28] D. A. Faroughy, A. Greljo, and J. Kamenik, Phys. Lett. B **764**, 126 (2017).
[29] A. Djouadi, T. Kohler, M. Spira, and J. Tutas, Z. Phys. C **46**, 679 (1990).
[30] D. Chakraverty, D. Choudhury, and A. Datta, Phys. Lett. B **506**, 103 (2001).
[31] K.-m. Cheung, Phys. Rev. D **64**, 033001 (2001).
[32] E. Coluccio Leskow, A. Crivellin, G. D'Ambrosio, and D. Mueller, Phys. Rev. D **95**, 055018 (2017).
[33] W. Altmannshofer, P. Stangl, and D. M. Straub, Phys. Rev. D **96**, 055008 (2017).
[34] G. D'Amico, M. Nardecchia, P. Panci, F. Sannino, A. Strumia, R. Torre, and A. Urbano, J. High Energy Phys. 09 (2017) 010.
[35] L.-S. Geng, B. Grinstein, S. Jaeger, J. Martin Camalich, X.-L. Ren, and R.-X. Shi, Phys. Rev. D **96**, 093006 (2017).
[36] M. Ciuchini, A. M. Coutinho, M. Fedele, E. Franco, A. Paul, L. Silvestrini, and M. Valli, Eur. Phys. J. C **77**, 688 (2017).
[37] G. Hiller and I. Nisandzic, Phys. Rev. D **96**, 035003 (2017).
[38] T. Hurth, F. Mahmoudi, D. Martinez Santos, and S. Neshatpour, Phys. Rev. D **96**, 095034 (2017).
[39] A. M. Baldini *et al.* (MEG), Eur. Phys. J. C **76**, 434 (2016).
[40] A. M. Baldini *et al.*, arXiv:1301.7225.
[41] Y. Amhis *et al.* (Heavy Flavor Averaging Group (HFAG)), arXiv:1412.7515.
[42] I. Doršner, S. Fajfer, A. Greljo, J. F. Kamenik, and N. Kosnik, Phys. Rep. **641**, 1 (2016).
[43] W. Buchmuller, R. Ruckl, and D. Wyler, Phys. Lett. B **191**, 442 (1987); **448**, 320(E) (1999).
[44] A. Crivellin, L. Hofer, J. Matias, U. Nierste, S. Pokorski, and J. Rosiek, Phys. Rev. D **92**, 054013 (2015).
[45] C. Biggio, M. Bordone, L. Di Luzio, and G. Ridolfi, J. High Energy Phys. 10 (2016) 002.
[46] S. Davidson, D. C. Bailey, and B. A. Campbell, Z. Phys. C **61**, 613 (1994).
[47] G. Couture and H. Konig, Phys. Rev. D **53**, 555 (1996).
[48] U. Mahanta, Eur. Phys. J. C **21**, 171 (2001).
[49] F. S. Queiroz, K. Sinha, and A. Strumia, Phys. Rev. D **91**, 035006 (2015).
[50] D. Das, C. Hati, G. Kumar, and N. Mahajan, Phys. Rev. D **94**, 055034 (2016).
[51] A. Blondel *et al.*, arXiv:1301.6113.
[52] B. Capdevila and J. Matias (private communication).